ISSN 1070-3284, Russian Journal of Coordination Chemistry, 2021, Vol. 47, No. 4, pp. 253–260. © Pleiades Publishing, Ltd., 2021.
Russian Text © The Author(s), 2021, published in Koordinatsionnaya Khimiya, 2021, Vol. 47, No. 4, pp. 218–225.

A New Metal-Organic Framework: Product of Solvothermal Synthesis in 3D-Printed Autoclaves

G. L. Denisov[a], P. V. Primakov[a, b], and Yu. V. Nelyubina[a, *]

[a] *Nesmeyanov Institute of Organoelement Compounds, Russian Academy of Sciences, Moscow, Russia*

[b] *Moscow State University, Moscow, Russia*

**e-mail: unelya@ineos.ac.ru*

Received August 28, 2020; revised October 26, 2020; accepted October 29, 2020

Abstract—A new metal-organic framework $\{Zn_4(BDC)_3(OAc)_2(DMF)_4\}$ (BDC = terephthalate anion) was synthesized under solvothermal conditions in a 3D-printed polypropylene autoclave. The product was isolated in a pure state and characterized by elemental analysis and X-ray diffraction (CIF file CCDC no. 2025811). The formation of this product, instead of the expected $\{Zn_4O(BDC)_3\}$ (MOF-5), was probably due to a change in the conditions of solvothermal synthesis caused by disruption of the integrity of the polypropylene autoclave. This is a drawback of this method of screening of metal-organic frameworks, which, however, in some cases givs rise to new representatives of this class of crystalline materials.

Keywords: 3D printing, autoclave, metal-organic framework, X-ray diffraction, solvothermal synthesis, zinc terephthalate

DOI: 10.1134/S1070328421040011

INTRODUCTION

Metal-organic frameworks (MOFs) [1] represent a unique class of crystalline materials featuring a periodic three-dimensional structure formed by metal ions or clusters and organic linkers coordinated to them [2]. The large internal surface area in combination with adjustable porosity [2] form the basis for their practical applications for gas storage [3] and separation [4], as proton-conducting membranes [5], as catalysts or their containers in various chemical processes [6], for targeted drug delivery [7], and even in structural biology [8]. Among the existing synthetic approaches [9] for the preparation of new metal-organic frameworks [9], a frequently used approach is solvothermal synthesis [10], which gives high-quality single crystals suitable for X-ray diffraction study of the crystal structure. For this purpose, the starting organic and inorganic components are heated in a high-boiling polar solvent up to temperatures that usually exceed the solvent boiling point [11] in commercially available metal autoclaves. These autoclaves are not only expensive and have definite dimensions (normally rather large), but they also require thorough cleaning after each experiment, which markedly reduces the efficiency of the high-throughput screening of MOFs [12].

As a solution to this problem, it was recently proposed to use 3D printing, an additive manufacturing technology [13], to fabricate autoclaves from polypropylene, which possesses the required chemical and thermal stability [14]. In recent years, 3D printing, suitable for producing monolithic plastic products by layer-by-layer extrusion of a polymer melt according to a 3D digital model [13] has acquired increasing popularity in chemical science for the manufacture of inexpensive research equipment [15–17], chemical reaction vessels [13, 14, 18, 19], and autoclaves for solvothermal synthesis of MOFs [14, 20]. Unlike conventional metal autoclaves, these autoclaves are inexpensive (having the price of the polypropylene filament [5]); hence, their fabrication for one-time use is not associated with significant financial expenditure, and their improper cleaning after the experiment cannot affect the subsequent syntheses. These autoclaves can have identical (or, conversely, different) dimensions, shapes, and other characteristics as desired by the researcher, and can be integrated into a common system to conduct parallel syntheses under identical conditions by analogy with multiwell plates [12]. Unfortunately, when 3D printing parameters or the design of polypropylene autoclaves are not optimized, the autoclaves may lose thermal stability [20], in some cases, even at temperatures below the polypropylene softening temperature (130–160°C depending on the polypropylene filament manufacturer [14]).

The purpose of this study is to produce a new MOF based on zinc(II) terephthalate, $\{Zn_4(BDC)_3(OAc)_2(DMF)_4\}$ (**I**) (BDC = terephthalate anion) by solvothermal synthesis [12, 21] under conditions used for the synthesis of the well known $\{Zn_4O(BDC)_3\}$

(a) (b)

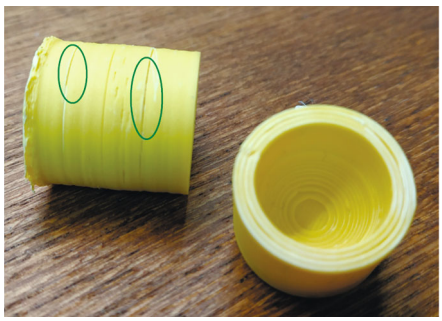

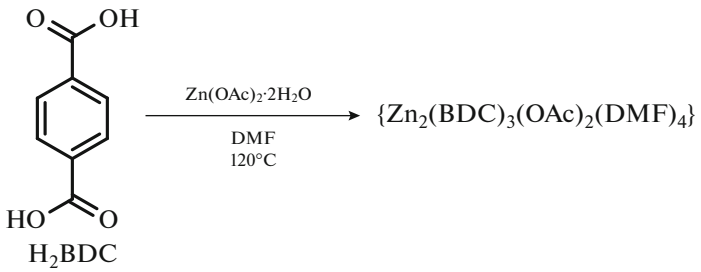

Fig. 1. (a) Polypropylene autoclave cut by a Dremel blade and (b) scheme of solvothermal synthesis of **I** (in Fig. 1a, the cracks formed in the autoclave after maintaining for 48 h at 120°C).

(MOF-5) (**II**) [1] using $Zn(OAc)_2 \cdot 2H_2O$ as the metal ion source [12, 22, 23] in a 3D printed polypropylene autoclave (Fig. 1). Product **I** was isolated in a pure state and characterized by elemental analysis and X-ray diffraction.

EXPERIMENTAL

All synthetic operations were performed in air using commercially available organic solvents and reagents (analytical grade). The analysis for carbon and hydrogen was carried out on a Carlo Erba model 1106 analyzer. Compound **I** was synthesized under conditions similar to those used in the previously described synthesis of MOF **II** [12].

Synthesis of complex I. $Zn(OAc)_2 \cdot 2H_2O$ (20.93 mg, 0.095 mmol) and H_2BDC (5.16 mg, 0.031 mmol) were dissolved/suspended in dry DMF (1 mL) using the automated device that we developed for dispensing liquid reagents (see below). This device was used to inject the reaction mixture into a 2.2 mL autoclave when 3D printing was 80% complete (see below) and, after that, printing was continued until the autoclave was hermetically sealed (4 h). The autoclave with the reaction mixture was heated to 120°C in a drying oven with programmable heating–cooling mode and kept at this temperature for 48 h. After cooling down to room temperature, the autoclave was opened by sawing along the polypropylene layers at a ~8 mm distance from the upper edge with a Dremel circular blade (Fig. 1a). The transparent prismatic single crystals suitable for X-ray diffraction that formed in the autoclave were separated from the mother liquor and washed in DMF (5 mL) for 24 h. Washing in $CHCl_3$ (5 mL) followed by drying on a rotary evaporator at room temperature for 2 h was repeated two more times. The yield of the product was 2.62 mg (23%).

For $C_{20}H_{23}N_2O_{10}Zn_2$

Anal. calcd., %	C, 41.26	H, 3.98	N, 4.81
Found, %	C, 41.39	H, 3.79	N, 4.92

Dispensing reactants and reaction mixture. Liquid reactants and the prepared reaction mixture were dispensed using the automated unit that we developed (Fig. 2), equipped with syringe pumps [8], which ensured high accuracy and a broad range of injected volumes (0.02 to 20 mL). The syringe pump tips were positioned using the mobile central platform of the unit designed as a 3D printer with delta geometry, characterized by high accuracy along all axes (up to 0.5 mm) and the possibility of fast replacement and modification of the platform, for example, to install additional equipment, at a lower cost compared to similar tooling for other 3D printers [9]. The stepper motors were driven by an Arduino Mega 2560 microcontroller [10] with the RAMPS attachment, version 1.4 [11], with Marlin free firmware [12]. The software for development of algorithms for platform positioning and dispensing liquid reactants and mixtures written in C++ language using the ImGui graphical interface library [13] allows the user to utilize pre-calculated reactant concentrations in a tabular form or enter a concentration range for automatic calculation. The resulting file with computer-readable GCODE commands [14] was processed with the Arduino microcontroller.

Manufacturing of the autoclave. The autoclave (Fig. 1) was 3D printed with engineering (yellow) syndiotactic FL-33 polypropylene with a softening temperature of 160°C [14], purchased from top3Dshop [24] as a standard 3D printing reel with wound polypropylene filament 1.75 mm in diameter (made in China; no other characteristics of the material are available). This material had a thermal and chemical (against various chemicals and solvents) stability [14] suitable for solvothermal synthesis of metal-organic frameworks (120°C, DMF). The parametric modeling of the autoclave was performed using OpenSCAD free software [25]; for 3D printing, the 3D model in the STL format [26] was converted to the G-code format [27] using the Simplify3D software [28]. Printing was carried out on a commercial Magnum Creative 2 UNI 3D printer [29] at the nozzle temperature of 248°C

and printing velocity of not more than 750 mm/min. A 5 mm-thick polypropylene board was used as the support.

X-ray diffraction study of the single crystal of **I** taken out from the autoclave immediately after cooling and opening was carried out at 120 K on a Bruker APEX2 DUO CCD diffractometer (MoK_α radiation, graphite monochromator, ω-scan mode). The structure was solved using the ShelXT program [15] and refined by the full-matrix least squares method on F^2_{hkl} with the Olex2 program [16] in the anisotropic approximation for non-hydrogen atoms. The positions of hydrogen atoms were calculated geometrically and refined in the isotropic approximation in the riding model. The main crystallographic data and refinement parameters of **I** are summarized in Table 1.

The full set of X-ray diffraction data for **I** was deposited with the Cambridge Crystallographic Data Centre (CCDC no. 2025811; http://www.ccdc.cam.ac.uk/). The topological analysis of MOF **I** was performed using the ToposPro program [21].

RESULTS AND DISCUSSION

We planned to carry out the solvothermal synthesis of the $\{Zn_4O(BDC)_3\}$ metal-organic framework (MOF-5) (**II**) by the previously described procedure [12], which was used for the high-throughput synthesis of this framework and included the dissolution of $Zn(OAc)_2{\cdot}2H_2O$ and H_2BDC in DMF (Fig. 1) and maintaining the reaction mixture for 48 h at 120°C in metal autoclaves [12] manufactured as 24-well plates. For expanding the opportunities offered by the proposed approach to the screening of MOFs, we chosen a 3D-printed polypropylene autoclave for the synthesis of **II** (Fig. 1). The reactants were dispensed with the automated unit that we developed (Fig. 2). The 3D printing of the autoclave was carried out using the printing parameters (concentric outer layers and serpentine type inner filling) and autoclave geometry (cylindrical shape with an outer spherical void and 4 mm thickness of all walls) optimized towards the conditions of solvothermal synthesis of MOFs in DMF at 120°C [14]. When the polypropylene autoclave was 80% complete, 3D printing was paused in order to introduce the reaction mixture by means of the automated dispensing unit (Fig. 2), and then printing was restarted until the autoclave was hermetically sealed [14].

The attempt to carry out the solvothermal synthesis of **II** (Fig. 1) in the polypropylene autoclave under the chosen conditions gave rise to transparent prismatic crystals. According to X-ray diffraction data (Table 1), this was previously unknown metal-organic framework based on zinc(II) terephthalate, $\{Zn_4(BDC)_3(OAc)_2(DMF)_4\}$ (**I**) (Figs. 3, 4). The nodes were formed by three symmetrically independent zinc(II) ions with different coordination environments com-

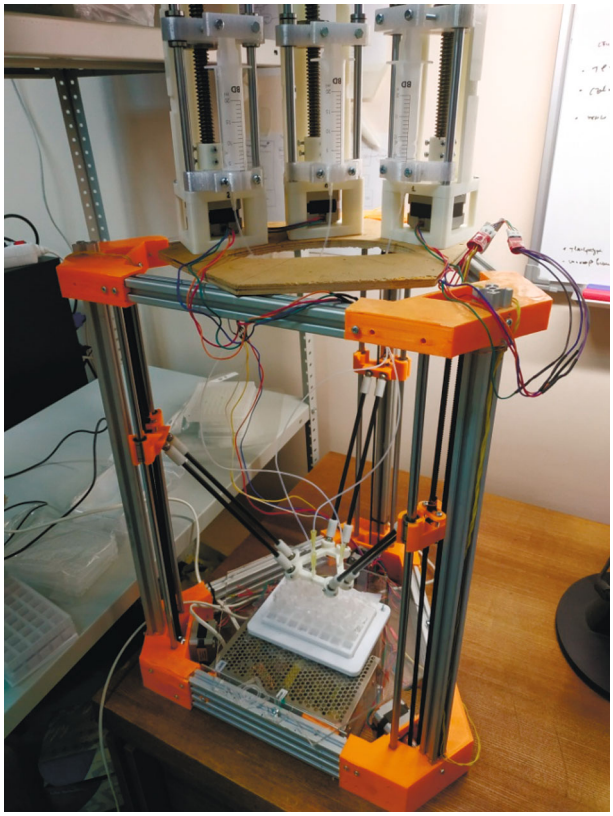

Fig. 2. Automated dispensing unit for liquid reactants and reaction mixtures.

posed of terephthalate and acetate anions and DMF molecules. The coordination polyhedra of two zinc ions (Zn(1) and Zn(3)), which occupied special positions (inversion centers) in the crystal, had a distorted octahedral geometry, whereas the third zinc(II) ion, which occupied the general position, had a pseudo-tetrahedral geometry (Table 2). For quantitative description of the polyhedra, we used the so-called "shape measures" [30], which characterize the deviation of their shape from the ideal octahedron (S(OC-6)) or tetrahedron (S(T-4)). The smaller these values, the better the geometry is described by the corresponding polyhedron. For the prepared metal-organic framework **I**, the S(OC-6) and S(T-4) values estimated from X-ray diffraction data using the Shape 2.1 software [30] are 0.043, 0.207, and 1.198 for zinc(II) ions in the (pseudo)octahedral and (pseudo)tetrahedral environments, respectively. The Zn(1) ion is connected to six terephthalate anions (Zn–O, 2.051(4)–2.193(3) Å), which are replaced in the case of Zn(3) by two acetate anions (Zn–O, 2.064(5) Å) and two DMF molecules (Zn–O, 2.095(3) 2.151(4) Å). The third zinc(II) ion is surrounded by only three terephthalate anions (Zn–O, 1.944(4)–2.015(3) Å) and one acetate anion (Zn–O, 1.974(4) Å). The described coordination bonds with terephthalate and acetate anions, which act as organic linkers, give rise to a metal-organic

Table 1. Key crystallographic data and structure refinement parameters for **I**

Parameters	Values
M	582.304
System	Monoclinic
Space group	$P2_1/c$
Z	4
a, Å	15.158(3)
b, Å	9.342(2)
c, Å	18.644(4)
β, deg	111.042(3)
V, Å^3	2463.9(9)
ρ(calcd.), g/cm^3	1.569
μ, cm^{-1}	2.002
F(000)	1911
$2\theta_{max}$, deg	52
Number of measured reflections	30894
Number of unique reflections	4565
Number of reflections with $I > 2\sigma(I)$	3240
Number of refined parameters	315
R_1 ($I > 2\sigma(I)$)	0.0560
wR_2 (for all data)	0.1520
GOOF	1.0634
Residual electron density (min/max), e Å^{-3}	−1.260/0.206

Table 2. Selected geometric parameters of the structure of **I**

Parameter*	Zn(1)	Zn(2)	Zn(3)
M–O_{BDC}, Å	2.051(4)–2.193(4)	1.943(4)–2.015(4)	
M–O_{OAc}, Å		1.974(4)	2.051(4)–2.193(4)
M–O_{DMF}, Å			2.095(4)–2.151(4)
S(OC-6)	0.043		0.207
S(T-4)		1.198	

* O_{BDC}, O_{OAc}, O_{DMF} are the oxygen atoms of terephthalate anions, acetate anions, and DMF molecules, respectively, S(OC-6) and S(T-4) are deviations of the shape of the metal ion polyhedron from the ideal octahedron (OC-6) and ideal tetrahedron (T-4), respectively.

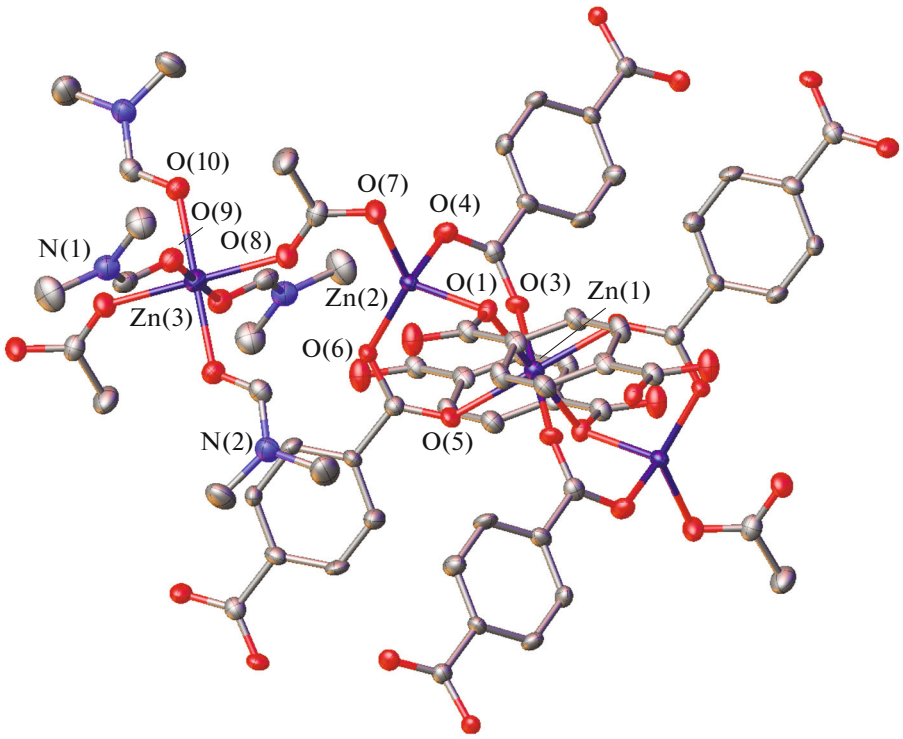

Fig. 3. Fragment of the crystal packing of **I** illustrating the coordination environment of zinc ions. The hydrogen atoms are omitted, the other atoms are shown as thermal ellipsoids ($p = 30\%$).

framework with triangular pores (Fig. 4) and with the solvent accessible volume of 925.95 Å^3 (found by processing of the X-ray diffraction data with the OLEX2 program [31]).

According to topological analysis of the crystal structure of **I** carried out using the ToposPro program [21], the MOF is formed by $\{Zn_3O_2(OOC)_6\}$ trimers coordinated by four terephthalate anions. The latter are, in turn, bound to only two $\{Zn_3O_2(OOC)_6\}$ trimers, i.e., they are bidentate and form layers parallel to the (1 0 0) crystallographic direction. The layers are linked to each other by bridging $\{ZnO_6\}$ monomers via common acetate anions, which are also bidentate, being linked to one $\{Zn_3O_2(OOC)_6\}$ trimer and one $\{ZnO_6\}$ monomer. In terms of the standard approach representing a MOF as a three-dimensional network [21], in which each $\{Zn_3O_2(OOC)_6\}$ trimer is considered as a single unit, the crystal packing of **I** is described by the known three-dimensional *hex* type hexagonal primitive network (8/3/h4) (Fig. 5), with the unit being designated as ($3^6.4^{18}.5^3.6$) [22].

The reason for the formation of **I** instead of the expected **II** is the change in the conditions of solvothermal synthesis (120°C, 1 mL of DMF) caused by disruption of the integrity of the polypropylene autoclave during long-term heating at 120°C (Fig. 1a), which we observed earlier in a similar synthesis of **II** [20], in which $Zn(NO_3)_2{\cdot}6H_2O$ served as the source of metal ions. In the latter case, this resulted in a mixture of two known reaction products, $\{Zn_4O(BDC)_3\}$ (MOF-5) [1] and $\{Zn_4O(BDC)_3\}{\cdot}(ZnO)_{0.125}$ (SUMOF-2) [32], whereas in the present study, we obtained an absolutely new metal-organic framework **I**. Unfortunately, it is unknown when the autoclave integrity was disrupted and, hence, our attempts to obtain this product once again by varying the authoclave wall thickness and volume, the reactant concentrations, and the residence time of the reaction mixture at 120°C failed.

Thus, under conditions meant for the solvothermal synthesis of $\{Zn_4O(BDC)_3\}$ (MOF-5) (**II**) (Fig. 1) in a 3D printed polypropylene autoclave, we obtained the previously unknown metal-organic framework $\{Zn_4(BDC)_3(OAc)_2(DMF)_4\}$ (**I**). The composition and structure of this product, formed instead of **II** due to the disruption of autoclave integrity during long-term heating, were confirmed by elemental analysis and X-ray diffraction. According to X-ray diffraction data, the crystal packing of **I** is described by the known three-dimensional *hex* type hexagonal primitive network (8/3/h4).

Although the use of polypropylene autoclaves makes it possible to perform solvothermal synthesis in an almost infinite number of identical autoclaves,

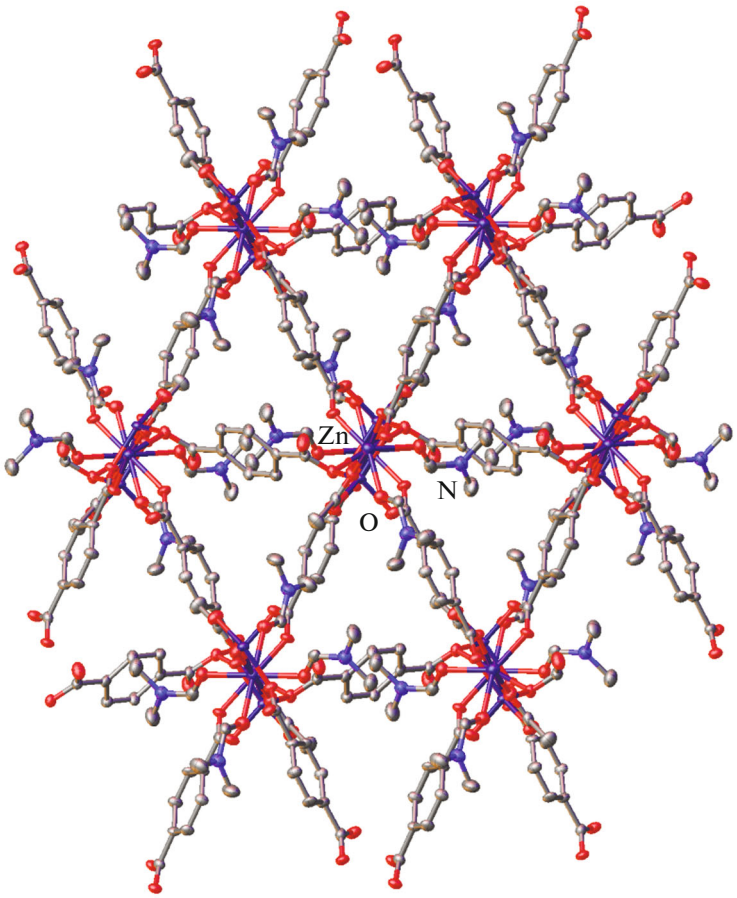

Fig. 4. Fragment of the crystal packing of **I** with atoms being drawn by thermal ellipsoids (p = 50%). The hydrogen atoms are omitted; the zinc ions and oxygen, nitrogen, and carbon atoms are shown.

characteristics of which (for example, the working volume, shape, and internal structure of the cavity) can be changed as desired by the researcher, their possible thermal instability even at temperatures below the softening point of polypropylene (130–160°C, depending on the manufacturer [14]) is a drawback of this approach for screening metal-organic frameworks. However, even this drawback, which can be solved if necessary [20] by selection of the appropriate characteristics of autoclaves (for example, wall thickness), makes it possible to obtain new representatives of this class of crystalline materials, thus providing wider opportunities for the search for metal-organic frameworks for various practical applications. Moreover, this opens up the potential for controlled rupture of an autoclave by 3D printing of thin membranes inside, in order to rapidly change the composition of the reaction mixture, and even perform the post-synthetic treatment of the product during a single solvothermal synthesis.

ACKNOWLEDGMENTS

The composition and structure of the product were studied using research equipment of the Center for Studies of Molecular Structure of the Nesmeyanov Institute of Organoelement Compounds, Russian Academy of Sciences, supported by the Ministry of Science and Higher Education of the Russian Federation.

FUNDING

This study was supported by the Russian Foundation for Basic Research (grant no. 19-29-08032). The design and manufacture of the automated unit for dispensing of reactants was supported by the Russian Foundation for Basic Research (grant no. 19-33-90260).

CONFLICT OF INTEREST

The authors declare that they have no conflicts of interest.

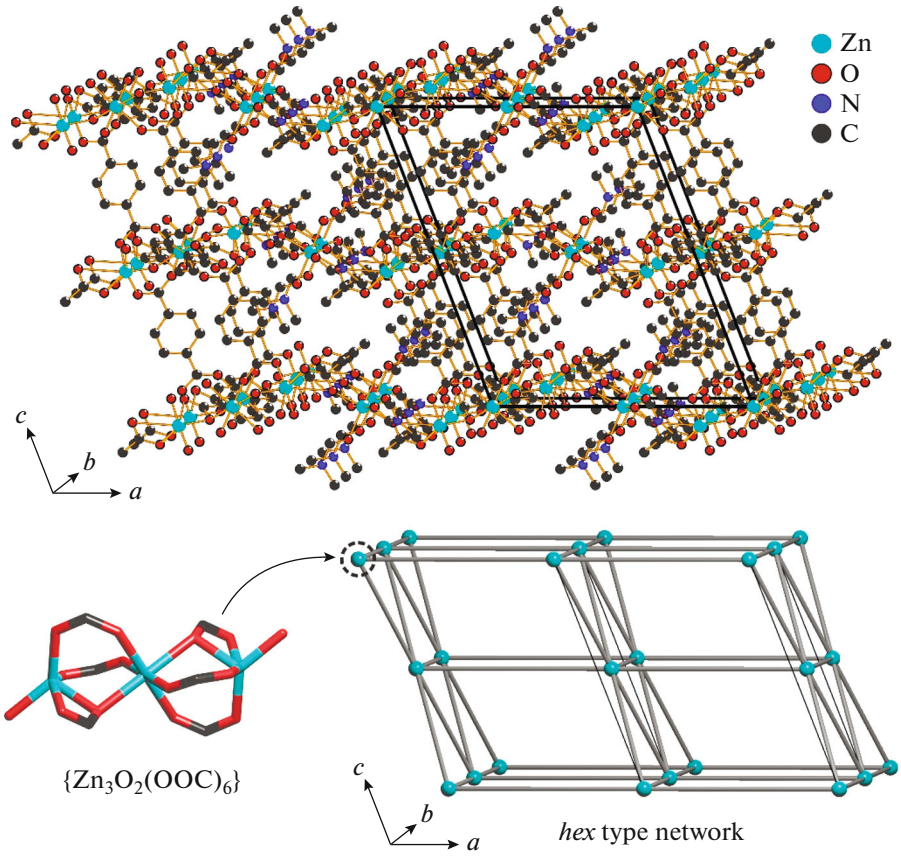

Fig. 5. Three-dimensional network with *hex* type topology in the crystal structure of **I**.

REFERENCES

1. Yaghi, O. and Li, H., *J. Am. Chem. Soc.*, 1995, vol. 117, no. 41, p. 10401.
2. Yaghi, O.M., O'Keeffe, M., Ockwig, N.W., et al., *Nature*, 2003, vol. 423, no. 6941, p. 705.
3. Wilmer, C.E., Leaf, M., Lee, C.Y., et al., *Nature Chem.*, 2012, vol. 4, no. 2, p. 83.
4. Herm, Z.R., Wiers, B.M., Mason, J.A., et al., *Science*, 2013, vol. 340, no. 6135, p. 960.
5. Yoon, M., Suh, K., Natarajan, S., and Kim, K., *Angew. Chem., Int. Ed. Engl.*, 2013, vol. 52, no. 10, p. 2688.
6. Lee, J., Farha, O.K., Roberts, J., et al., *Chem. Soc. Rev.*, 2009, vol. 38, no. 5, p. 1450.
7. Giménez-Marqués, M., Hidalgo, T., Serre, C., and Horcajada, P., *Coord. Chem. Rev.*, 2016, vol. 307, p. 342.
8. Inokuma, Y., Yoshioka, S., Ariyoshi, J., et al., *Nature*, 2013, vol. 495, no. 7442, p. 461.
9. Stock, N. and Biswas, S., *Chem. Rev.*, 2011, vol. 112, no. 2, p. 933.
10. Zhao, Y., Li, K., and Li, J., *Z. Nature B*, 2010, vol. 65, no. 8, p. 976.
11. Chen, X.-M. and Tong, M.-L., *Acc. Chem. Res.*, 2007, vol. 4, no. 2, p. 162.
12. Biemmi, E., Christian, S., Stock, N., and Bein, T., *Microporous Mesoporous Mater.*, 2009, vol. 117, no. 1, p. 111.
13. Gordeev, E., Degtyareva, E., Ananikov, V., *Izv. Akad. Nauk, Ser. Khim.*, 2016, no. 6, p. 1637.
14. Kitson, P.J., Marshall, R.J., Long, D., et al., *Angew. Chem., Int. Ed. Engl.*, 2014, vol. 53, no. 47, p. 12723.
15. Zhang, C., Wijnen, B., and Pearce, J.M., *J. Lab. Autom.*, 2016, vol. 21, no. 4, p. 517.
16. Baden, T., Chagas, A.M., Gage, G., et al., *PLoS Biology*, 2015, vol. 13, no. 3, p. e1002086.
17. Berman, B., *Business Horizons*, 2012, vol. 55, no. 2, p. 155.
18. Kitson, P.J., Glatzel, S., Chen, W., et al., *Nature Protocols*, 2016, vol. 11, no. 5, p. 920.
19. Symes, M.D., Kitson, P.J., Yan, J., et al., *Nature Chem.*, 2012, vol. 4, no. 5, p. 349.
20. Denisov, G.L., Primakov, P.V., Korlyukov, A.A., et al., *Russ. J. Coord. Chem.*, 2019, vol. 45, p. 836. https://doi.org/10.1134/S1070328419120030
21. Hajiashrafi, S. and Motakef Kazemi, N., *Heliyon*, 2019, vol. 5, no. 9, p. e02152.
22. Biserčić M.S., Marjanović B., Vasiljević B.N., et al., *Microporous Mesoporous Mater.*, 2019, vol. 278, p. 23.
23. Tranchemontagne, D.J., Hunt, J.R., and Yaghi, O.M., *Tetrahedron*, 2008, vol. 64, no. 36, p. 8553.
24. Top3DShop. https://top3dshop.ru/.

25. *OpenSCAD. The Programmers Solid 3D CAD Modeller.* https://www.openscad.org/documentation.html2009.

26. Koc, B., Ma, Y., and Lee, Y.-S., *Rapid Prototyping J.*, 2000, vol. 6, no. 3, p. 186.

27. *CNC Control Setup for Milling and Turning: Mastering CNC Control Systems*, Smid, P., Ed., Industrial Press Inc., 2010.

28. Simplify3D Software. https://www.simplify3d.com/software/documentation/.

29. 3D Printers, Magnum. https://magnum3d.ru/.

30. Alvarez, S., *Chem. Rev.*, 2015, vol. 115, p. 13447.

31. Bourhis, L.J., Dolomanov, O.V., Gildea, R.J., et al., *Acta Crysrtallogr, Sect. A: Found. Adv.*, 2015, vol. 71, no. 1, p. 59.

32. Yao, Q., Su, J., Cheung, O., et al., *J. Mat. Chem.*, 2012, vol. 22, no. 20, p. 10345.

Translated by Z. Svitanko